UDC 539.4

Properties and Applications of the Electrohydraulic Servosystem of the Hydraulic Excavator

W. H. Jia,[a,1] C. B. Yin,[b] G. Li,[a] C. L. Sun,[a] C. Wang,[a] and H. Feng[b]

[a] School of Mechanical Engineering, Nanjing Institute of Technology, Jiangsu, China

[b] School of Mechanical and Power Engineering, Nanjing University of Technology, Jiangsu, China

[1] geovrml@163.com

The service of a hydraulic excavator is complicated by poor environment. The safety and stability of the control system are influenced by external factors. The object of the study is the electrohydraulic servosystem of the hydraulic excavator. The mathematical and simulation models using AMESIM for the servosystem are constructed. Then the pressure and flow characteristics are analyzed. The design and optimization of the electrohydraulic servosystem and its application in excavator engineering are described. The operation process is graphically presented by a curve, which steeply slopes up (rising period) and then flattens out (stabilization period), those periods are shortened by 38.0 and 40.5%, respectively, the delay tracking period decreased by 52.6%, and anti-interference is reliable.

Keywords: electrohydraulic system, delay tracking period, anti-interference, safety and stability.

Introduction. As a key part of engineering machinery, hydraulic excavators have been widely used in construction, transportation, and disaster rescue operations, due to their superior efficiency. However, the complicated working conditions and harsh working environment of hydraulic excavators have proposed higher requirements for their intelligent control. By combining hydraulic and electrical control technologies, the electrohydraulic servosystem facilitates hydraulic excavators [1–3] in remote control, self-operation, and synergetic work via this integrated control.

This study proposes a simulation model for electrohydraulic servosystem and investigates its pressure and flow responses. A mathematical model of this servosystem is proposed based on the force balance, voltage, and flow equations. Moreover, the stability of electrohydraulic servosystem is studied using the Bode plot and the Nichols diagram.

In this paper, using AMESIM, discretion of outlet pressure vs. displacement curve leads to a series of data. The outlet displacement parameters were set by data input via the prescribed route. The main valve, which is indeed a combination of multi-link three-position, six-way valve, is subdivided into several basic functional units, and modules of these units were established using corresponding modules in the hydraulic element database: BAO21 and BAO22 modules were used for the main body of slide valve, BAP12 module was used for the pilot control chamber, MAS005 module was used to characterize the mass of spool and the viscous friction experienced by spool, LSTP00A and MCLSPL00AA spring modules were used to establish the center spring.

The scheme of the control system used in this study is shown in Fig. 1a, where *1* is arm cylinder, *2* is electrohydraulic servovalve, *3* is main platform, *4* is valve pump, *5* is rotary motor, *6* is boom cylinder, and *7* is bucket. Photos of pressure/temperature sensors and data acquisition system are presented in Fig.1b and 1c, respectively.

The input electrical signal is amplified and transduced to the electrohydraulic servovalve, the spool shifts, the hydraulic pump initiates, resulting in displacement of the hydraulic cylinder. The output signal is then transduced to by the displacement sensor a feedback electrical signal, which is then compared to the command signal to obtain the bias

© W. H. JIA, C. B. YIN, G. LI, C. L. SUN, C. WANG, H. FENG, 2018

a b c

Fig. 1. Excavator structure diagram.

voltage signal. The latter is transmitted to the servovalve via the amplifier. The servovalve then controls the hydraulic actuator to reduce the bias between the output and command signals within a preset range [4, 5]. In this way, a closed-loop control is achieved.

The composition of electrohydraulic servocontrol system is shown in Fig. 2, where *1* is valve pump, *2* is one-way valve, *3* is overflow valve, *4* is electrohydraulic servovalve, *5* is hydraulic bucket cylinder, *6* is displacement sensor, *7* is load, and *8* is servoamplifier).

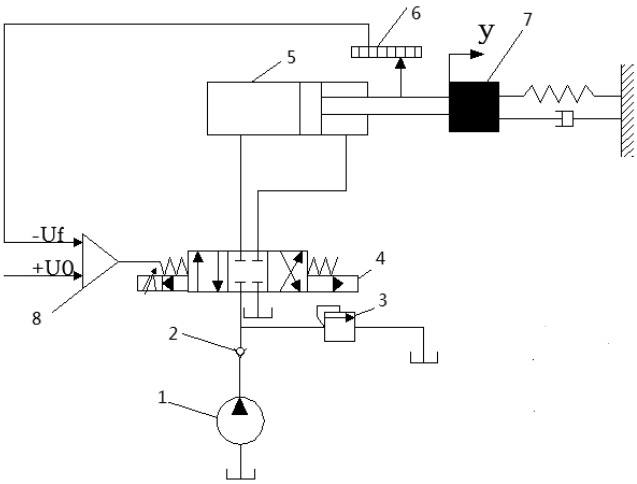

Fig. 2. Schematic structure of excavator.

1. Mathematical Model of Electrohydraulic Servosystem.

1.1. Servoamplifier. The bias control signal (Δu) was generated by the comparison element based on input and feed-back signals. As the amplification element, the servo amplifier amplifies Δu, which is relatively weak, to realize the control of the electrohydraulic servovalve [6, 7]. The transfer function is as follows:

$$I(s) = K_1 U(s), \tag{1}$$

where I is the input current to the electrohydraulic servovalve, U is the voltage signal generated by the servo amplifier, and K_1 is the amplification coefficient.

1.2. Electrohydraulic servovalve. A displacement feedback servovalve consists of a moving coil force motor, control slide valve, and main valve. With current flowing through, the coil in the motor generates an electromagnetic force to push the control slide valve, the

top and bottom throttle shifts, and the main valve shifts. Once the displacement of the control slide valve and that of the main spool are aligned, the valve does not move further.

1.3. Moving Coil Force Motor. The signal voltage on the control coil by the servo amplifier is the sum of the voltage drop on the resistor, self-induced back electromotive force in the control coil, and the back electromotive force induced by movement of control coil in the magnetic field. The voltage balance equation is as follows:

$$E = (R_c + r_p)i + L_c dt_c/dt + K_b dx/dt, \tag{2}$$

where R_c is the resistance of the control coil, r_p is the internal resistance of the amplifier, L_c is the inductance of the control coil, and K_b is the back electromotive force constant ($K_b = B_g \pi D d N_c$).

The force balance equation for coil component is as follows:

$$F = m d^2x/dt^2 + B\, dx/dt + Kx, \tag{3}$$

where m is the mass of coil, B is the damping coefficient of coil, and K is the spring stiffness.

Laplace transform of Eqs. (2) and (3) results in

$$I_c = (K_1 U - K_b sX)/((R_c - r_p)(1 + s/\varpi_\alpha)), \tag{4}$$

where ϖ_α is the corner frequency of the control coil ($\varpi_\alpha = (R_c + r_p)/L_c$)$\delta_0 = B/2\sqrt{1/km}$, $\varpi_0 = \sqrt{k/m}$,

$$X/I_c = (K_t/K)/(s^2/\varpi_0^2 + 2\delta_0/\varpi_0 s + 1). \tag{5}$$

1.4. Control Slide Valve - Main Valve. The masses of front slide valve and main valve are m_1 and m_2 the dynamic damping coefficients of front slide valve and main valve are c_1 and c_2, the spring stiffness of front slide valve and main valve are K_a and K_b, and the flow gain of front slide valve is K_{qp}. The force balance equation for front slide valve and main valve is as follows:

$$F_1 = m_1\, d^2x/dt^2 + c_1\, dx/dt + K_{qp} x_v, \tag{6}$$

$$F_2 = m_2\, d^2x_v/dt^2 + c_2\, dx_v/dt + K_b x_v - \Delta P_x A_v. \tag{7}$$

The open capacity of front slide valve can be determined by

$$x_e = x - x_v. \tag{8}$$

Excluding the effects of flow force, the transfer function can be obtained based on Eqs. (6)–(8):

$$x_v/x_e = (K_{qp}/A_v)/(s(s^2/\omega_{hp}^2 + 2s\delta_{hp}/\omega_{hp} + 1)), \tag{9}$$

$$x_v/x = 1/((s/K_v + 1)(s^2/\omega_{hp}^2 + 2s\delta_{hp}/\omega_{hp} + 1)). \tag{10}$$

The simplified block diagram of transfer equation of direct location feedback servovalve is shown in Fig. 3.

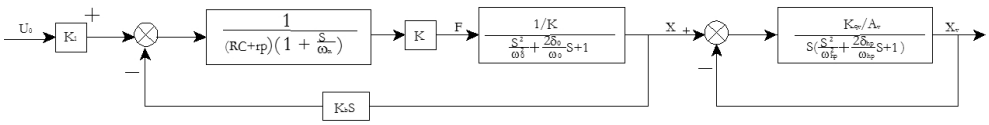

Fig. 3. Diagram of transfer equation of direct location feed-back servovalve.

Hydraulic Cylinder – Load. Assuming that the pressure in the hydraulic cylinder is uniform, the temperature and bulk modulus of hydraulic medium are constant and the leakage of hydraulic cylinder is laminar flow. The flow equation of electrohydraulic servovalve is as follows:

$$Q_L = K_q x_v - K_c p_L . \tag{11}$$

If the piston is located in the middle part, the system stability is poor, the frequency of hydraulic component is low, and the damping ratio is low. Also, $V_1 = V_2 = V_t/2$ is valid in the hydraulic cylinder. The overall leakage coefficient ($C_{tp} = C_{ip} + C_{ep}/2$) is used to reflect the effect of hydraulic cylinder leakage on the load flow. The flow in the hydraulic cylinder can be determined by

$$Q_L = A_p\, dx_p/dt - C_{tp}\, p_L + v_t/4\beta \cdot dp_t/dt, \tag{12}$$

where A_p is the effective area of the piston (m^2), x_p is the displacement of the piston (m), C_{ip} is the leakage coefficient of the hydraulic cylinder (m$^3 \cdot$s^{-1}/Pa), and β is the effective bulk modulus (Pa).

The force balance equation for hydraulic cylinder is as follows:

$$A_p Q_L = m_t\, d^2 x_p \big/ dt^2 - B\, dx_p/dt + K x_p + F_L , \tag{13}$$

where m_t is the overall mass of piston (kg), F_L is the external load on the piston (N), and K_{ce} is the overall flow-pressure coefficient, $K_{ce} = K_c + C_{tp}$.

Equations (11)–(13) are equations for displacement, pressure, and flow of the hydraulic cylinder, respectively. These parameters are indicators of dynamic performance of the hydraulic cylinder. Laplace transform of these equations results in overall displacement of the piston in the hydraulic cylinder:

$$x_p = (K_q/A_p x_v - K_{ce}\big/A_p^2\,(1 + sV_t/(4\beta K_{ce})F_L))\big/(m_t V_t)(4\beta A_p^2 s^3 + ((m_t K_{ce})\big/A_p^2 +$$

$$+ (BV_t)\big/(4\beta A_p^2))s^2 + (((BK_{ce})\big/A_p^2) + (KV_t)\big/(4\beta A_p^2) + 1) + KK_{ce}\big/A_p^2). \tag{14}$$

2. Modeling of Electrohydraulic Servosystem.

2.1. Establish System Modeling. In the electrohydraulic servo [8–11], the hydraulic cylinder pushes the load, the displacement sensor at the load converts location signal to electrical signal. The bias between the actual location signal and the designated location signal is amplified and applied on the electrohydraulic servovalve. The servo spool shifts, the flow of hydraulic system fluctuates, and the location of hydraulic cylinder is adjusted to achieve trajectory tracking.

The flow is defined as 0 when the servovalve is at the initial position. The flow is defined as $+1$ at an extreme position. Herein, Port P is connected to Port A and Port T is connected to Port B. The flow is defined as -1 at the other extreme position. Herein, Port A is connected to Port T and Port B is connected to Port P.

2.2. Step Signal Comparison. The key component parameters of the simulation model are summarized in Table 1. The values of these parameters were determined based on the actual system. The signal set-up of the signal source: the signal stays at 0 in 0~1 s, increased to 0.8 in 1~4 s, and stays at 0.8 in 4~6 s. To test the dynamic characteristics of the system, typical step signals were employed as standard displacement signals. The reference value of step signal was set to be 0.1 m. Figure 4 shows step signal displacement curves obtained by traditional control system and servo control system, respectively.

T a b l e 1

System Parameters

Motor rated speed (rpm)	1500
Pump rated displacement (cm^3/rev)	122
Pump speed (rpm)	1500
Rated current of servovalve (mA)	200
Natural frequency (Hz)	50
Damping ratio	1
Servoamplifier gain	250
Diameter of hydraulic cylinder piston (mm)	120
Diameter of hydraulic cylinder piston rod (mm)	85
Piston block mass (kg)	100
Cylinder stroke (m)	1

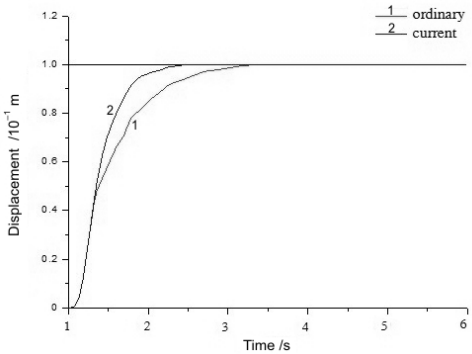

Fig. 4

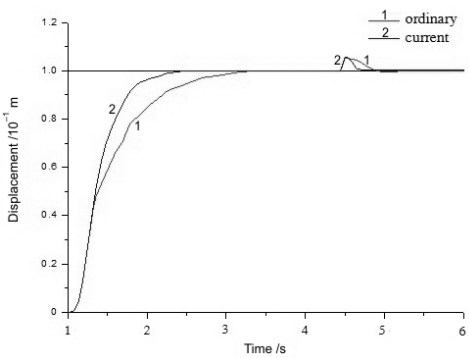

Fig. 5

Fig. 4. Displacement response curve of step signal.
Fig. 5. Displacement response curve of undesired signal.

As observed, the steady-state errors in both cases approached 0, while the system rise durations were 1.96 and 1.59 s, and the system stabilization durations were 3.36 and 2.41 s. The rise duration and stabilization duration of output step signal decrease by 38 and 40.5%, respectively, indicating improved output performance (fast response).

2.3. Anti-Interference Performance. To simulate excavator loading, non-restoring interference signals were involved. The interference signal, whose amplitude was 5% of signal amplitude, was added at $t = 4.5$ s, as shown in Fig. 5.

As observed, the adjustment duration of the servosystem to interference signals was 0.32 s, while that of traditional system was 1.6 s and fluctuations were observed.

3. Performance Analysis of Servovalve Control Cylinder. Simulation and analysis of electrohydraulic servo. The simulation time is set to be 6 s to check the steady operation status of the system. The communication interval is set to be 0.01 s to exclude effects of system fluctuations. The pressure and flow of key components were obtained and analyzed.

Figure 6 shows the flow curve in the hydraulic cylinder. During 0~1 s, the electrical signal is 0, the servovalve is closed, and the flow in the hydraulic cylinder is 0. After 1 s, an electrical signal is observed, the servovalve shifts, and flows in rod-containing cavity and rodless cavity vary. At the initial stage, the flow in rod-containing cavity varies smoothly, while that in rodless cavity varies drastically. After 2.4 s, fluctuations of flows in both cavities approach negligible. Eventually, the maximum flows in rodless cavity and rod-containing cavity are 8.66 and 4.33 l/min, respectively. Figure 7 shows the pressure in the hydraulic cylinder.

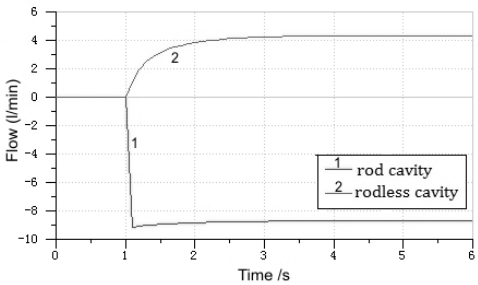

Fig. 6. Flow curve in the hydraulic cylinder.

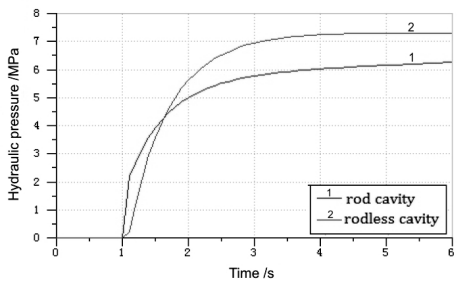

Fig. 7. Pressure in the hydraulic cylinder.

Figure 8 shows the displacement of servovalve spool as a function of time. Once the electrical signal is observed, the valve opens and reached the extreme position at 1.2 s.

Figure 9 shows the flow curve at the pump valve outlet. Once the hydraulic system is initiated, the outlet flow is maintained at 183 l/min. During 0~1 s, the electrical signal is 0 and the flow at the overflow valve increases drastically to 183 l/min. After 1 s, an electrical signal is observed, the servovalve shifts, and the flow at the overflow valve decreases gradually. As the spool of servovalve reached the extreme position, the flow at the overflow valve stays at 174.3 l/min.

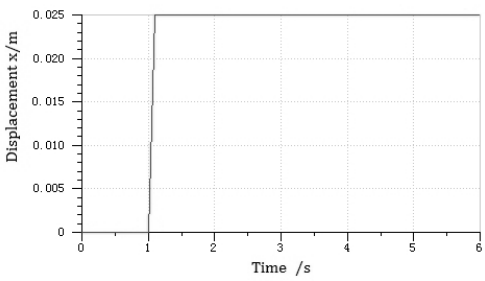

Fig. 8. Displacement of servovalve spool.

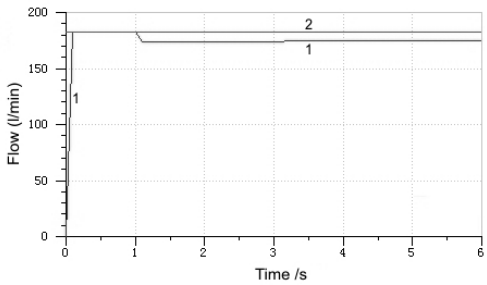

Fig. 9. Flow curve at the pump valve outlet: 1-rod cavity, 2 -rodless cavity.

Conclusions. A mathematic model of the servosystem of valve-control excavator cylinder was established. With step signal and combination of step signal and impulse interference signal as the reference displacement signal, fast response capability, tracking capability, and anti-interference capability were studied. The results indicated that the rising and stabilization periods decreased by 38 and 40.5%, respectively, the delay tracking period

dropped by 52.6%, and excellent anti-interference was observed. Once the servosystem approached the steady state, the maximum pressure of rod cavity reached 7.28 MPa, while the maximum and outlet flows corresponded to 4.33 and 174.3 l/min, respectively.

1. C. Liu, Z. Tang, X. Zhao, and Z. Pey, "The modeling and simulation study of hydraulic intelligent power system based on AMESim," in: Proc. of the Guidance, Navigation and Control Conference (CGNCC), 2014 IEEE Chinese (August 8–10, 2014, Yantai, China), IEEE (2014), DOI: 10.1109/CGNCC.2014.7007419.
2. Y. Ye, C. B. Yin,Y. Gong, and J. J. Zhou, "Position control of nonlinear hydraulic system using an improved PSO based PID controller," *Mech. Syst. Signal Pr.*, **83**, 241–259 (2017).
3. W. Jia, C. Yin, D. Zhu, and X. Jiang, "Influence of rectangular grooved labyrinth seal on the flow characteristics of valve core," *J. Comput. Theor. Nanos.*, **13**, No. 4, 2376–2381 (2016).
4. N. Xie, X. Chen, and J. J. Guo, "Simulation analysis of proportional valve controlled cylinder hydraulic system based on AMESim," *Adv. Mater.s Res.*, **668**, 420–425 (2013).
5. W. Jia, C. Yin, B. Jia, et al., "Application research on the dual-spool valve control system in a hydraulic farm-oriented load tractor," *INMATEH – Agricult. Eng.*, **48**, No. 1, 103–112 (2016).
6. R. Amirante, L. A. Catalano, and P. Tamburrano, "The importance of a full 3D fluid dynamic analysis to evaluate the flow forces in a hydraulic directional proportional valve," *Eng. Computation.*, **31**, No. 5, 898–922 (2014).
7. L. L. Li, L. Q. Huo, Q. Zhang, and B. Sun, "Design and simulation analysis of servo amplifier," *Process Automat. Instr.*, **33**, No. 12, 83–85 (2012).
8. A. Tivay, M. Zareinejad, S. M. Rezaei, and K. Baghestan, "A switched energy saving position controller for variable-pressure electrohydraulic servosystems," *ISA T.*, **53**, No. 4, 1297–1306 (2014).
9. M. H. Chiang, L. W. Lee, and H. H. Liu, "Adaptive fuzzy controller with self-tuning fuzzy sliding-mode compensation for position control of an electrohydraulic displacement-controlled system," *J. Intell. Fuzzy Syst.*, **26**, No. 2, 815–830 (2014).
10. V. Milić, Z. Situm, and M. Essert, "Robust H-infinity position con trol synthesis of an electrohydraulic servosystem," *ISA T.*, **49**, No. 4, 535–542 (2010).
11. K. Baghestan, S. M. Rezaei, H. A. Talebi, and M. Zareinejad, "An energy-saving nonlinear position control strategy for electrohydraulic servosystems," *ISA T.*, **59**, 268–279 (2015).

Received 15. 09. 2017